Molecular Dynamics Simulations of Curcumin in the Interface Region of Triblock Copolymer Micelles

K. P. K. Luft, S. Gekle

published in

NIC Symposium 2020
M. Müller, K. Binder, A. Trautmann (Editors)

Forschungszentrum Jülich GmbH,
John von Neumann Institute for Computing (NIC),
Schriften des Forschungszentrums Jülich, NIC Series, Vol. 50,
ISBN 978-3-95806-443-0, pp. 289.
http://hdl.handle.net/2128/24435

Molecular Dynamics Simulations of Curcumin in the Interface Region of Triblock Copolymer Micelles

Konstantin P. K. Luft and Stephan Gekle

Biofluid Simulation and Modeling, Theoretische Physik VI, Universität Bayreuth, 95440 Bayreuth, Germany
E-mail: {konstantin.luft, stephan.gekle}@uni-bayreuth.de

In this work we present the results of an orientation analysis of a single tautomeric curcumin molecule in water and polymeric melts of poly(2-oxazoline) and poly(2-oxazine) based triblock copolymers. The results yield stacking of the aromatic phenyl rings for curcumin solvated in water, while showing that the molecule is mostly prolate when solvated in the polymeric melts. The comparison of curcumin in the two different triblock copolymers however showed no significant difference in the two observed reaction coordinates d and θ.

1 Introduction

Efficient delivery of drug molecules to patients is a major problem. In most cases, drug transportation cannot simply be achieved in an aqueous solution, since the majority of modern drugs have very poor water solubility, but requires some sort of carrier molecule which needs to have both, hydrophilic and hydrophobic parts, to be able to dissolve the drug molecules. Two examples of such hydrophobic drugs are paclitaxel (PTX) and curcumin (CUR), with water solubilities of $5.56\,\mathrm{mg/L}$[9] and $5.75\,\mathrm{mg/L}$,[10] respectively.

Lübtow *et al.*[1] showed a comparison of the maximal drug concentration of these drugs achievable in ABA triblock copolymers based on a hydrophilic part **A**, consisting of poly(2-methyl-2-oxazoline) (pMeOx), and a hydrophobic part **B**, consisting of poly(2-oxazoline) (pOx) or poly(2-oxazine) based polymers (pOzi), namely poly(2-n-propyl-2-oxazoline) (pPrOx), poly(2-butyl-2-oxazoline) (pBuOx), poly(2-n-propyl-2-oxazine) (pPrOzi) and poly(2-n-butyl-2-oxazine) (pBuOzi), of which two can be seen in Fig. 1. Surprisingly, they found that the structural isomers **ApBuOxA** and **ApPrOziA** showed the biggest difference in solubility for the different drugs.

While **ApBuOxA** achieved the best PTX drug loading of $\approx\ 48\,\mathrm{wt\,\%}$, **ApPrOziA** showed the second worst drug loading of approximately $25\,\mathrm{wt\,\%}$, corresponding to a drug concentration of $\rho_{\mathrm{PTX}} = 9.04 \pm 0.61\,\mathrm{g/L}$ and $\rho_{\mathrm{PTX}} = 3.27 \pm 0.01\,\mathrm{g/L}$, respectively, for a polymer concentration of $\rho_p = 10\,\mathrm{g/L}$. The same test for CUR displayed a significantly different behaviour, as it showed the highest drug loading of $\approx\ 54\mathrm{wt\,\%}$ with the polymer **ApPrOziA** and yielded the worst drug loading of $\approx 24\,\mathrm{wt\,\%}$ in combination with **ApBuOxA**, again with a polymer concentration of $\rho_p = 10\,\mathrm{g/L}$ and corresponding to a curcumin concentration of $\rho_{\mathrm{CUR}} = 11.91 \pm 0.59\,\mathrm{g/L}$ and $\rho_{\mathrm{CUR}} = 3.23 \pm 0.18\,\mathrm{g/L}$, respectively.[1]

Schulz *et al.*[2] did research on the morphological properties of similar copolymers with PTX loading, which yielded that the polymer-drug-macromolecular structure forms spherical micelles, with a size of 10 to $25\,\mathrm{nm}$, even at small drug loadings in aqueous solutions. The structural model proposed by Pöppler *et al.*[3] gives a deeper insight into the

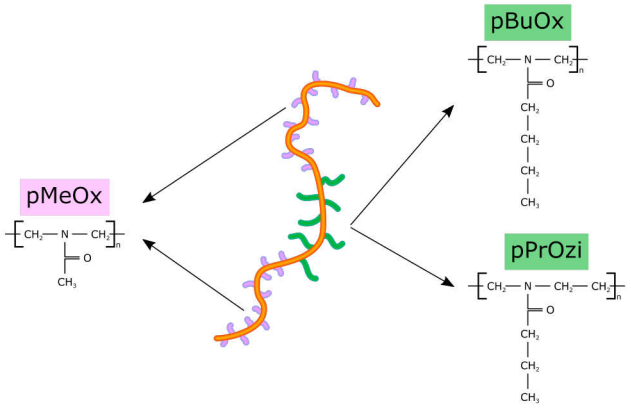

Figure 1. Schematic representation of two of the polymers used by Lübtow *et al.*[1]

properties within the micelles incorporating CUR molecules. The model states that at low drug loadings all drug molecules are present in the hydrophobic core, while the hydrophilic shell of the micelle is filled with water. As the drug loading increases, the core fills up and the drug molecules settle in the hydrophilic part, extruding water from the shell.

2 Simulation Methods and Systems

System Construction

Our particular interest is the difference in drug loading of the two structural isomers (ApPrOziA and ApBuOxA).[1] To get an idea of the origin of this difference, we used Molecular Dynamics to simulate a small sample system using **ApPrOziA** and **ApBuOxA** polymers and one curcumin molecule in a cubic volume with $a \approx 3.7\,\mathrm{nm}$ edge length. The small system size was chosen to represent a small volume within the interface region between the hydrophilic and hydrophobic parts of the polymer micelle. Due to the lack of water in this region as proposed by Pöppler *et al.*,[3] a polymeric melt was chosen to approximate the polymer movement within the micelles.

The copolymers used in the experiments of Pöppler *et al.*[3] had repeating units of $38{-}23{-}38$ for A-B-A, respectively. To generate the needed *GROMOS 54A7* forcefields, ATb[4, 11–14] was used. The restrictions for ATb's semi-empirical forcefields only allowed molecules with a maximum size of 500 atoms, thus the repeating units had to be adjusted. The hydrophilic/hydrophobic ratio of the experimentally used polymers is $\eta_{\mathrm{exp}} \approx 1.65$. To make most use of the limitation, repeating units of $11{-}7{-}11$ for A-B-A, respectively, were chosen for the simulations, resulting in a ratio of $\eta_{\mathrm{sim}} \approx 1.57$.

In nature, curcumin is a tautomeric molecule, existing in a diketo and in a keto-enol form (see Fig. 2). Manolova *et al.*[5] showed, that the keto-enol form of curcumin is the common form in organic solvents, while the diketo form is rare in this environment. With an increasing percentage of water in a mixture of organic solvents and water, the diketo

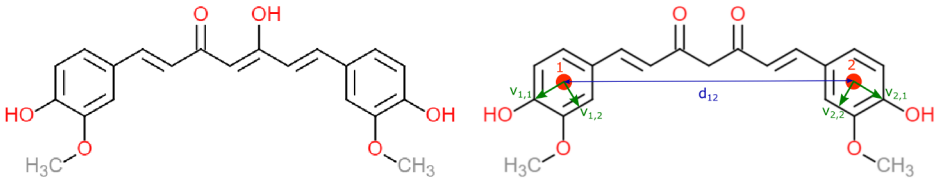

(a) Keto-enol

(b) Diketo

Figure 2. Illustration of the two tautomeric forms of curcumin, (a) showing the keto-enol form, (b) shows a schematic representation of the values obtained using the diketo from of curcumin as an example. The COM's, symbolised by the red dots, are used to calculate the distance d and also to calculate the vectors $\vec{v}_{i,j}$, which span the plane of the carbon rings.

form appears more frequent. We decided to simulate both forms of curcumin to achieve a better understanding of what happens within the micelles.

To characterise the system we looked at two reaction coordinates, namely the COM (centre of mass) distance d of the two carbon rings and the angle θ_{12} between the normal vectors of the planes created by the phenyl rings (see Fig. 2). The COM was calculated by using only the six carbon atoms per ring and neglecting the hydroxy and OMe rest, while the angle was calculated by

$$\theta_{12} = \frac{\vec{n}_1 \cdot \vec{n}_2}{|\vec{n}_1| \cdot |\vec{n}_2|} \tag{1}$$

with $\vec{n}_i = \vec{v}_{i,1} \times \vec{v}_{i,2}$.

Due to the OMe group of the phenyl ring, a difference in direction of $\vec{n}_i$ can be determined. Using both parameters one can determine the geometrical configuration of curcumin, which can then be used to generate a 2-dimensional configuration space.

Simulation Sequence

All simulations were done using *GROMACS 2018.1*[6–8] and analysed using the GROMACS analysis template. Each simulation used a time step of $dt = 1\,\text{fs}$, the trajectories were written every $\Delta t = 1\,\text{ps}$.

We built one aqueous system with a single curcumin molecule in diketo form and water using the *solvate* command in *GROMACS* to fill a box with edge length $a = 3\,\text{nm}$. This system was initialised using energy minimisation and a NPT-Ensemble run at a temperature of $T = 400\,\text{K}$ for $t = 10\,\text{ns}$. After the initialisation we obtained 300 start configurations from the trajectory, which were equally distributed within the configurations space (see Fig 4(a)).

The polymer systems were built using the *GROMACS* function *insert-molecules*, by inserting 12 polymer molecules and one of the two curcumin forms in a cubic box with edge length $a = 7\,\text{nm}$, thus creating four systems **PrOzi-Keto**, **BuOx-Keto**, **PrOzi-Enol**

and **BuOx-Enol**. A flow chart of the simulations used to obtain all needed results of the polymer systems can be seen in Fig. 3.

The start configurations were first simulated in an initialisation run consisting of an energy minimisation, followed by a run in a NVT-Ensemble, with a temperature of $T = 700\,\mathrm{K}$ for $t = 500\,\mathrm{ps}$, and a NPT-Ensemble simulation at the same temperature for $t = 30\,\mathrm{ns}$. The high temperature was chosen to allow the long polymer molecules to move faster, the NVT-Ensemble simulation allows the polymers move freely, while the simulation in the NPT-Ensemble lets them compress and entangle, thus achieving a better equilibration and greater structural difference from the start configuration of the polymers, compared to a NPT-run at 300 K for the same duration. The trajectory obtained by the NPT-run of the initialisation was used to search for different geometrical configurations of curcumin, equally distributed within the configuration space, which resulted in about 80 to 85 start configurations per initialisation run. For all systems the start configurations were then again minimised and used as start configuration in NPT-Ensemble simulations at $T = 300\,\mathrm{K}$ with a simulation time of 30 ns and 10 ns for the polymer melts and water, respectively. The resulting trajectories were then analysed and for each time frame the

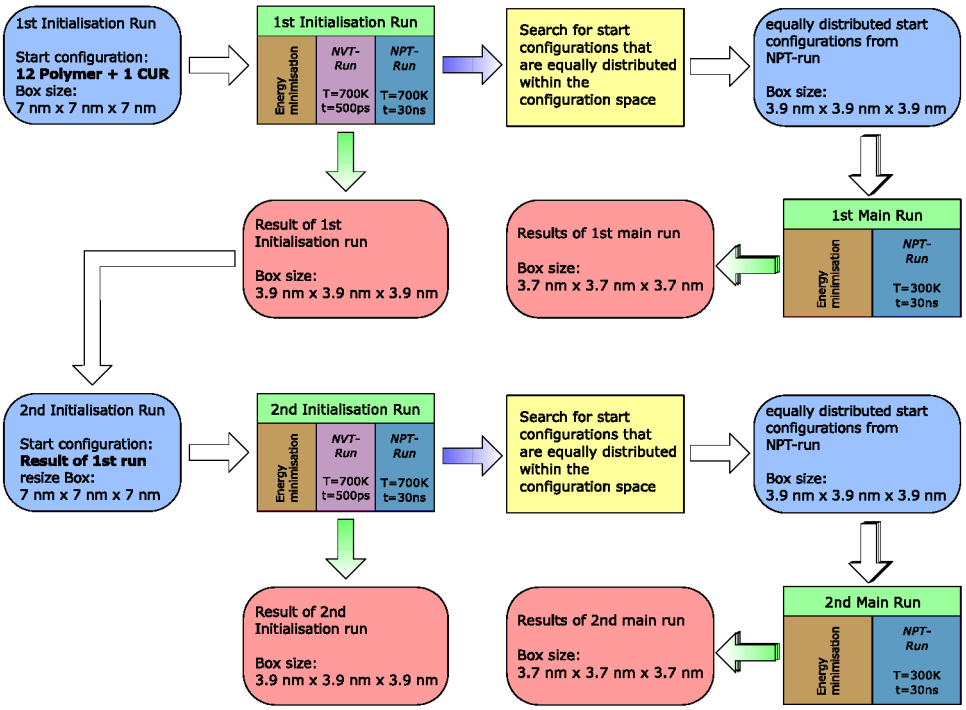

Figure 3. Flow chart of the simulation sequence. The blue rectangles with rounded corners represent the start configurations used, the red rectangles with rounded corners represent the results obtained. The rectangles with green title are showing the separate simulations used within one run (from left to right), while the yellow rectangles represent the program used to find start configurations. The green gradient arrows show that the result is obtained at the end of the run, while the blue gradient arrows show, that the trajectory obtained by the NPT-run was used in the next step.

configuration was saved in a two dimensional histogram with bin sizes $B_{\text{angle}} = 0.5°$ and $B_{\text{distance}} = 2.5\,\text{pm}$ (see Figs. 4 and 5).

We used this pattern two times per system, using the result of the first initialisation run to start the second initialisation. To rule out the difference of the polymer configurations in the original initialisation of the systems, when comparing the diketo and the keto-enol forms of curcumin, a program was used to change one form into the other. This way we got four different starting points per system, where the only difference of the *Polymer*-Keto and *Polymer*-Enol systems is the form of curcumin and not the orientation of the polymers.

3 Results and Discussion

The results obtained from the simulation of the aqueous system displayed in a two dimensional configuration space plot can be seen in Fig. 4(b). One can see two prominent regions (P1 and P2) in configuration space, where P1 is at an angle of $\theta_{1,aq} \approx 170°$ and a distance of $d_{1,aq} \approx 0.4\,\text{nm}$ and P2 at $\theta_{2,aq} \approx 10°$ and $d_{2,aq} \approx 0.4\,\text{nm}$. By comparing the two regions one can see that P1 is slightly more prominent than P2. These two configurations correspond to two $\pi - \pi-$stacking forms of CUR's phenyl rings, where the P2 configuration is less frequent, due to the OMe groups of the two rings being next to each other, which can result in a separation of the rings when the OMe groups turn towards one another. In P1 on the other hand, the OMe groups are on opposite sites of the stacked rings and can thus not separate the rings easily, resulting in a higher stability of the P1 configuration. We also observed flipping from one state into the other, resulting in the fine, slightly bent line between the two peaks. The bent line is due to the flipping mostly involving the OMe group of one ring stacking onto the other ring, thus creating a bigger distance between the two rings centre of masses.

The results obtained from the four polymer systems however display a completely different behaviour of CUR compared to the aqueous system. Instead of two precise peaks in the configuration space plots, one can observe a much broader variety of configurations (see Fig. 5). The purple areas in Fig. 5(a)-(d) show the less often found configurations,

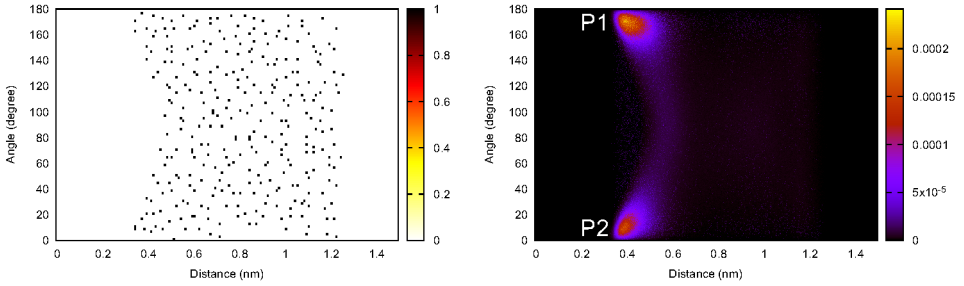

(a) Start configurations (b) Configuration Space

Figure 4. Configuration space plots of the water system, (a) shows the distribution of 300 start configurations within the configuration space, (b) shows the result of the start configurations after 10 ns of NPT-simulation, displaying two peaks P1 (upper peak) and P2 (lower peak).

which seem to be mostly found in CUR molecules moving towards a more prominent configuration. These configurations are displayed by two prominent regions, one at a distance of $d_{1,p} \approx 0.6\,\text{nm}$, the other at distances between $0.8\,nm$ and $1.2\,nm$. The system PrOzi-Keto additionally shows smaller peaks in the same positions as the P1 and P2 peaks in the aqueous system, as can be seen in Fig. 5(b), which again represent $\pi - \pi-$stacking of curcumin's phenyl rings. Further, when comparing the BuOx systems (Fig. 5(a) and (c)) to the PrOzi systems (Fig. 5(b) and (d)), one can see that the PrOzi system displays more confined areas in the configuration space.

However, the difference of the prominent configurations between the two polymers is not significant enough to be the sole reason for better solubility of CUR in ApPrOziA. A comparison of the diketo and keto-enol forms, both within the same polymer, yields that the prominent peaks of the keto-enol forms exhibit a more stretched form in angle direction, while the diketo form displays broader stretching in direction of the distance variable. This can be explained by the difference in bonding of both forms. While the keto-enol form is more planar due to the C-C double bond in the molecules middle part between the oxygen atoms (see Fig. 2(a)), and thus being less able to fold but moving by torsion. The diketo form on the other hand does not have a C-C double bond in the middle part, allowing it to fold more freely (see Fig. 2(b)).

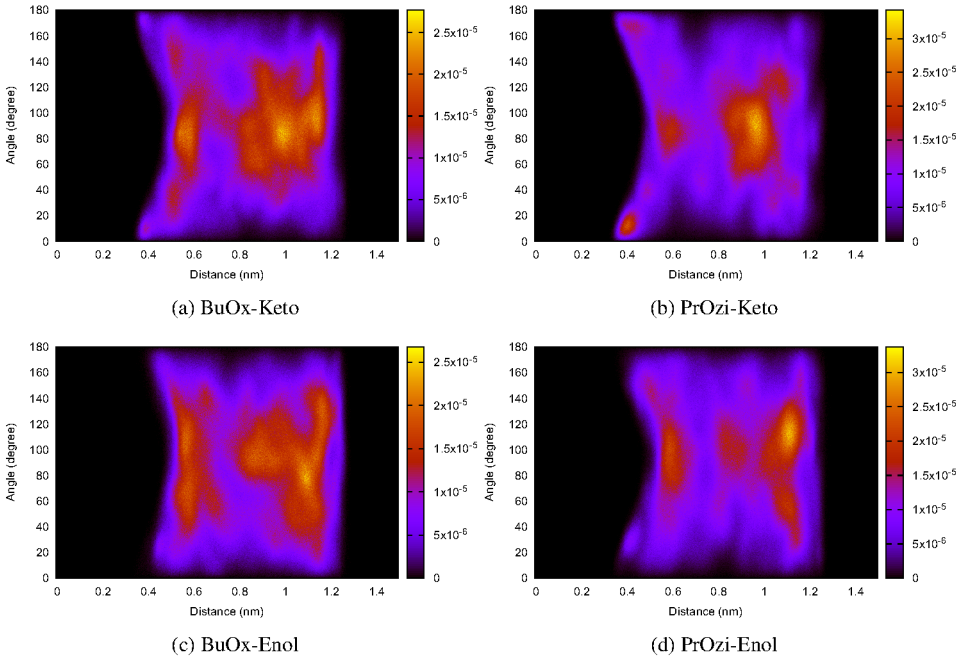

(a) BuOx-Keto

(b) PrOzi-Keto

(c) BuOx-Enol

(d) PrOzi-Enol

Figure 5. Configuration space plots of the polymer systems, (a) shows curcumin in diketo form dissolved in ApBuOxA, (b) the diketo form dissolved in ApPrOziA, (c) the keto-enol form dissolved in ApBuOxA, and (d) the keto-enol form dissolved in ApPrOziA.

4 Conclusion

The simulations done in this work give an impression of how a single curcumin molecule is incorporated within the interface region of triblock copolymer micelles and its orientation in different solutions. While the results of our simulations were able to show a difference in orientation for curcumin solvated in water (stacking of the aromatic phenyl rings) and curcumin in polymeric melt (mostly showing a prolated form), it could not show significant differences when comparing the orientation of curcumin in ApBuOxA and ApPrOziA, thus not confirming the findings of Lübtow *et al.*[1]

A possible reason for this could be that the diffusion time of the polymeric melt is too large to get viable results by simulations as short as 30 ns. By using single curcumin molecules instead of multiple ones we also stray far from the concentration achieved by Lübtow *et al.*[1] and therefore neglect possible curcumin-curcumin interactions, which could also stabilise the micelle and increase drug loading. Taking the structural model for these specific polymer micelles proposed by Pöppler *et al.*[3] into account, simulations of the core and corona regions and comparisons of the different regions could also yield important informations for understanding the high drug loading ability of ApPrOziA, which will be investigated in the future.

Another way to find differences in the two polymer systems could be the radial distribution of different functional groups of the polymers in respect to functional groups of curcumin, since the keto-enol form exhibits an additional hydrogen bond donor, that could possibly alter the way in which the functional groups of the polymers move.

Acknowledgements

The authors gratefully acknowledge the computing time granted by the Jülich Supercomputing Centre (JSC).

This work was funded by the Deutsche Forschungsgemeinschaft (DFG, German Research Foundation) - Projektnummer 326998133 - TRR 225 (subproject B07). Special thanks belong to Robert Luxenhofer for useful discussions.

References

1. M. M. Lübtow, L. Hahn, M. S. Haider, and R. Luxenhofer, *Drug Specificity, Synergy and Antagonism in Ultrahigh Capacity Poly(2-oxazoline)/Poly(2-oxazine) based Formulations*, J. Am. Chem. Soc. **139**, 10980–10983, 2017.
2. A. Schulz, S. Jaksch, R. Schubel, E. Wegener, Z. Di, Y. Han, A. Meister, J. Kressler, A. V. Kabanov, R. Luxenhofer, C. M. Papadakis, and R. Jordan, *Drug-Induced Morphology Switch in Drug Delivery Systems Based on Poly(2-oxazoline)s*, ACS Nano **8**, 2686–2696, 2014.
3. A.-C. Pöppler, M. M. Lübtow, J. Schlauersbach, J. Wiest, L. Meinel, and R. Luxenhofer, *Loading Dependent Structural Model of Polymeric Micelles by Solid-State NMR*, Preprint,2019, doi:10.26434/chemrxiv.8943251.v1.
4. A. K. Malde, L. Zuo, M. Breeze, M. Stroet, D. Poger, P. C. Nair, C. Oostenbrink, and A. E. Mark, *An Automated Force Field Topology Builder (ATB) and Repository: Version 1.0*, Journal of Chemical Theory and Computation **7**, 4026–4037, 2011.

5. Y. Manolova, V. Deneva, L. Antonov, E. Drakalska, D. Momekova, and N. Lambov, *The effect of the water on the curcumin tautomerism: A quantitative approach*, Spectrochimica Acta Part A: Molecular and Biomolecular Spectroscopy **132**, 815–820, 2014.
6. E. Lindahl, B. Hess, and D. van der Spoel, *GROMACS 3.0: A package for molecular simulation and trajectory analysis*, J. Mol. Mod. **7**, 306–317, 2001.
7. S. Páll, M. J. Abraham, C. Kutzner, B. Hess, and E. Lindahl, *Tackling exascale software challenges in molecular dynamics simulati ons with GROMACS*, Solving Software Challenges for Exascale **8759**, 3–27, 2015.
8. M. J. Abraham, T. Murtola, R. Schulz, S. Páll, J. C. Smith, B. Hess, and E. Lindahl, *GROMACS: High performance molecular simulations through multi-level parallelism from laptops to supercomputers*, SoftwareX **1**, 19–25, 2015.
9. `https://www.drugbank.ca/drugs/DB01229`
10. `https://www.drugbank.ca/drugs/DB11672`
11. `https://atb.uq.edu.au/molecule.py?molid=275982`
12. `https://atb.uq.edu.au/molecule.py?molid=8102`
13. `https://atb.uq.edu.au/molecule.py?molid=359238`
14. `https://atb.uq.edu.au/molecule.py?molid=350170`